Extended-Distance Wireless Power Transfer System With Constant Output Power and Transfer Efficiency Based on Parity-Time-Symmetric Principle

Xujian Shu, Bo Zhang, *Senior Member, IEEE*, Zhihao Wei, Chao Rong, and Shubin Sun

***Abstract*—Maintaining constant power transfer while keeping near-unity transfer efficiency at varying transfer distances is a major challenge for existing wireless power transfer (WPT) system with multiple repeaters. In order to overcome the problem, this article proposes a novel WPT mechanism with multiple repeaters based on the concept of parity-time symmetry. First, the coupled-mode model of this WPT relay system is established. Then, the steady-state transfer characteristics of the proposed WPT system with an odd and even number of repeaters are analyzed. The theoretical analysis shows that whether an odd or even number of repeaters are inserted between the transmitting and receiving coils, the proposed system automatically achieves constant output power and transfer efficiency against the variation of the transfer distance without any tuning or feedback within a certain distance. The prototype with one repeater and two repeaters is implemented to verify the validity of the theoretical analysis. Experimental results show that the prototype with one repeater can transfer power with an invariant transfer efficiency of 91% and a constant output power of 15 W within a transfer distance of 420 mm. Similarly, the prototype with two repeaters transfers constant power of 15 W over a transfer distance ranging from 420 to 500 mm, and the transfer efficiency is constant near 89%.**

***Index Terms*—Constant output power, constant transfer efficiency, parity-time (PT) symmetric, repeater, wireless power transfer (WPT).**

I. Introduction

IN RECENT decades, due to the benefits of high reliability, convenience, and safety, the WPT technology has developed rapidly and widely, especially magnetic coupling resonance wireless power transfer (MCR-WPT) technology. In 2007, Kurs *et al.* [1] first introduced the coupled-mode theory (CMT) into the modeling and analysis of MCR-WPT system, and successfully lit a 60 W bulb without any wire connections over a distance in excess of 2 m based on the principle of MCR, which was published in *Science*. Although the transfer efficiency dropped from 70% to 45% when the transfer distance expanded from 1.5 to 2 m, the publication of this research result is still a significant breakthrough in WPT technology, which has aroused great interest in academia and industry. Subsequently, a large number of researches on WPT have been published, and the WPT has been thoroughly investigated in various applications, including mobile phones chargers [2]–[4], electric vehicles charging [5]–[7], and biomedical implants charging [8]–[10]. However, the traditional WPT system is not robust against variation of transfer distance and misalignment between coils [1], [11], which has brought a significant challenge for the practical applications of the WPT technology. To ensure stable and efficient power transfer, several strategies have been proposed, including resonant frequency tracking [12], [13], adding multiple intermediate coils to realize adaptive impedance matching [14], [15], using metamaterials to magnify the near field [16], and introducing the concept of parity-time (PT) symmetry to achieve nonlinear tuning [17], [18].

Indeed, optimizing the transfer efficiency of WPT systems at varying distances is the focus of most existing researches. PT symmetry provides a good idea to address this issue. The concept of PT symmetry originates from quantum mechanics [19], and the PT-symmetric system is defined by invariance under the combined P- and T-reversal, where P-reversal means spatial inversion, T-reversal consists of inverting the flow of time. This concept was later introduced into optics [20], photonics [21], acoustics [22], and electric circuits [23]. In 2017, PT symmetry was first introduced into the WPT system with a two-coil structure by Assawaworrarit *et al*. [17]. When the PT-symmetric conditions are satisfied, a near-unity power transfer efficiency that is insensitive to the coupling coefficient is achieved in the exact PT-symmetric region.

Furthermore, as one of the fundamental approaches to increase the operating distance, the system with repeaters can significantly improve its transfer efficiency compared with that of the two-coil scheme. Recently, a number of studies of WPT relay systems have been undertaken. For instance, Oh [24] analyzed the influence of the intermediate coil on the voltage transfer function of the WPT system, and presented an output voltage regulation method by adding additional wireless serial communication modules, which increase the complexity of system design. Wen *et al.* [25] used the multiobjective optimization

Manuscript received August 23, 2020; revised December 26, 2020; accepted January 27, 2021. Date of publication February 3, 2021; date of current version May 5, 2021. This work was supported by the Key Program of the National Natural Science Foundation of China under Grant 51437005. Recommended for publication by Associate Editor A. Safaee. *(Corresponding author: Bo Zhang.)*

The authors are with the School of Electric Power, South China University of Technology, Guangzhou 510641, China (e-mail: epshuxujian@163.com; epbzhang@scut.edu.cn; hankwei0722@163.com; eprongchao@mail.scut.edu.cn; 201821014654@mail.scut.edu.cn).

Color versions of one or more figures in this article are available at https://doi.org/10.1109/TPEL.2021.3056538.

Digital Object Identifier 10.1109/TPEL.2021.3056538

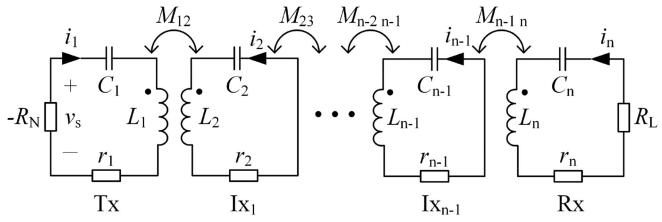

Fig. 1. Schematic of the proposed nonlinear PT-symmetric-based WPT relay system.

algorithm to optimize the parameters of the relay coil to improve the transfer efficiency, but the calculation is complicated. Kim *et al.* [26] analyzed a symmetric three-coil WPT system using the CMT and showed that the optimum position for a repeater to maximize the output power is the center between the transmitting coil (Tx) and receiving coil (Rx). The authors of [27]–[29] compared the system energy efficiency of two- and three-coil WPT systems, and showed that the three-coil WPT system could achieve higher system energy efficiency and lower sensitivity to load change. Moon *et al.* [30] proposed a high-efficiency WPT system with an asymmetric four-coil resonator, which uses two intermediate coils on the primary side to boost the apparent coupling coefficient, thereby improving the transfer efficiency. Liu *et al.* [31] proposed a coupling coefficient tuning scheme for a WPT system with double intermediate resonators to maximize the power transfer efficiency, in which the calculation is complicated and the shape of the coil is restricted. However, the above existing work mainly focuses on optimizing the transfer characteristics for the fixed operating condition. When the transfer distance changes or the coils are misaligned, the transfer efficiency and output power deteriorated seriously. Therefore, it is difficult for the conventional WPT relay system to operate stably and efficiently at varying transfer distances or misalignment.

In this article, a generalized PT-symmetric-based WPT system with multiple repeaters is proposed, in which not only the operating distance is improved, but also the output power and transfer efficiency remain constant under a misalignment or variation of the transfer distance, thereby guaranteeing stable and efficient power transfer. In Section II, the coupled-mode model (CMM) of the proposed WPT relay system is established. The PT-symmetric conditions for the system with an odd number of repeaters are deduced, and the characteristics, including the operating frequency, output power, critical coupling coefficient, and transfer efficiency are analyzed in Section III. Similarly, Section IV derived the PT-symmetric conditions and analyzed the transfer characteristics of the system with an even number of repeaters. Then, a 15 W prototype is implemented and tested to validate the validity of the theoretical analysis in Section V. Finally, the conclusion is given in Section VI.

II. System Structure and Modeling

The WPT system with multiple repeaters based on the nonlinear PT-symmetric model is proposed, as shown in Fig. 1. Here, $-R_N$ is a negative resistance that is used as a power source to provide input voltage v_s to the system. L_1, L_2, …, and L_n are the self-inductances of the coils. r_1, r_2, …, and r_n are the internal resistances of the coils. C_1, C_2, …, and C_n are the tuning capacitances. M_{12}, M_{23}, and $M_{n-1\,n}$ are mutual inductances between adjacent coils. Generally, for a WPT relay system, compared with the strong coupling coefficients between two adjacent coils k_{n-1} ($=M_{n-1n}/\sqrt{L_{n-1}L_n}$, $n=2, 3, \ldots$), the coupling coefficients between nonadjacent coils that are far away from each other can be negligible, i.e., k_{ij} ($=M_{ij}/\sqrt{L_iL_j}$) $\approx$ 0 (i = 1, 2, …, n − 2; $j = i + 2, i + 3, \ldots, n$). $M_{n-1\ n}$ is the mutual inductance between n-1th and nth adjacent coils, M_{ij} is the mutual inductance between the ith and jth nonadjacent coils. Finally, considering that both the inductive load and the capacitive load can be expressed in the form of impedance, which only affects the specific expressions of the natural frequency and load rate of the receiver, the form of the coupled-mode equation remains unchanged. Without loss of generality, we only consider purely resistive load, that is, R_L is the equivalent load resistance.

According to the dynamic modeling method of CMM [32], the dynamic equations of the proposed WPT system with multiple repeaters can be derived as

$$\frac{\mathrm{d}}{\mathrm{d}t}\begin{bmatrix}\boldsymbol{a}_1\\ \boldsymbol{a}_2\\ \boldsymbol{a}_3\\ \vdots\\ \boldsymbol{a}_n\end{bmatrix} = \begin{bmatrix} \mathrm{j}\omega_1 - \frac{\tau_1}{2} + g & -\mathrm{j}\frac{\omega_2 k_1}{2} & 0 & \cdots & 0\\ -\mathrm{j}\frac{\omega_1 k_1}{2} & \mathrm{j}\omega_2 - \frac{\tau_2}{2} & -\mathrm{j}\frac{\omega_3 k_2}{2} & \cdots & 0\\ 0 & -\mathrm{j}\frac{\omega_2 k_2}{2} & \mathrm{j}\omega_3 - \frac{\tau_3}{2} & \cdots & 0\\ \vdots & \vdots & \vdots & \ddots & \vdots\\ 0 & 0 & 0 & \cdots & \mathrm{j}\omega_n - \frac{\tau_{nL}}{2}\end{bmatrix}\begin{bmatrix}\boldsymbol{a}_1\\ \boldsymbol{a}_2\\ \boldsymbol{a}_3\\ \vdots\\ \boldsymbol{a}_n\end{bmatrix}. \tag{1}$$

Here, the subscript n (= 1, 2, …) denote the oscillators of Tx, intermediate coils (Ix_1, Ix_2, …), and Rx, respectively. $\boldsymbol{a}_n = \frac{1}{2}\sqrt{L_n}(i_n \pm \mathrm{j}\omega_n C_n u_{Cn})$ are coupled modes, which are defined so that the energy contained in the oscillator n is $|\boldsymbol{a}_n|^2$. $\omega_n = 1/\sqrt{L_nC_n}$ are natural resonant frequencies of oscillators. i_n are the currents flowing through the coils L_n, u_{Cn} are the voltages across the tuning capacitances C_n. $\tau_n = r_n/L_n$ are internal loss rates of oscillators, $\tau_L = R_L/L_n$ is the load rate, $\tau_{nL} = \tau_n + \tau_L$. $g = V_s/(2\sqrt{L_1}|\boldsymbol{a}_1|)$ is the gain rate of Tx, which depends on the module value $|\boldsymbol{a}_1|$ and the root-mean-square (rms) value V_s of input voltage v_s.

III. Analysis of PT-Symmetric Model of System With an Odd Number of Repeaters

The system in which the dynamic model is invariant with respect to the combined P- and T-reversal is PT-symmetric. Such systems are generally accomplished by adding balanced energy gain and loss mechanisms. In electricity, the P-reversal is equivalent to exchanging labels corresponding to pairs of associated circuit components. T-reversal only requires modification of the resistor due to its dissipative nature. When the circuit

parameters of a system satisfy the PT-symmetric conditions, the energy stored in the transmitting oscillator remains equal to the energy stored in the receiving oscillator, i.e., the power provided by the gain is absorbed completely by the load and the internal resistances, typically resulting in constant transfer efficiency [17], [18].

Taking one repeater as an example to obtain the PT-symmetric model and analyze the transfer characteristics of the three-coil WPT relay system, which can be generalized into the WPT relay system with an odd number of repeaters. For a complete energy transfer, the natural resonant frequencies of Tx, Ix_1, and Rx should be close, i.e., $\omega_1 \approx \omega_2 \approx \omega_3 = \omega_0$ [33]. Considering that the repeater Ix_1 mainly plays the role of widening the transfer distance, its internal resistances r_2 is small enough to be ignored. And the maximum efficiency can be achieved for the case that the Ix_1 is located in the center between Tx and Rx [26]. Thus, supposing that $r_2 \approx 0$ and $k_1 = k_2 = k_m$, the coupled-mode equations of the proposed WPT relay system with one repeater can be rearranged as

$$\frac{\mathrm{d}}{\mathrm{d}t}\begin{bmatrix}\boldsymbol{a}_1\\ \boldsymbol{a}_2\\ \boldsymbol{a}_3\end{bmatrix} = \begin{bmatrix}\mathrm{j}\omega_0 - \frac{\tau_1}{2} + g & -\mathrm{j}\frac{\omega_0 k_m}{2} & 0\\ -\mathrm{j}\frac{\omega_0 k_m}{2} & \mathrm{j}\omega_0 & -\mathrm{j}\frac{\omega_0 k_m}{2}\\ 0 & -\mathrm{j}\frac{\omega_0 k_m}{2} & \mathrm{j}\omega_0 - \frac{\tau_{3L}}{2}\end{bmatrix}\begin{bmatrix}\boldsymbol{a}_1\\ \boldsymbol{a}_2\\ \boldsymbol{a}_3\end{bmatrix}. \tag{2}$$

Assuming that the steady solutions are the form $[\boldsymbol{a}_1, \boldsymbol{a}_2, \boldsymbol{a}_3]^T = [A_1, A_2, A_3]^T e^{\mathrm{j}\omega t}$, A_n $(n = 1, 2, 3)$ are the amplitudes of $\boldsymbol{a}_n$, ω is the operating frequency of the three-coil WPT relay system, which is determined by the characteristic equation as follows:

$$\begin{vmatrix}\mathrm{j}(\omega-\omega_0) + \frac{\tau_1}{2} - g & \mathrm{j}\omega_0\frac{k_m}{2} & 0\\ \mathrm{j}\omega_0\frac{k_m}{2} & \mathrm{j}(\omega-\omega_0) & \mathrm{j}\omega_0\frac{k_m}{2}\\ 0 & \mathrm{j}\omega_0\frac{k_m}{2} & \mathrm{j}(\omega-\omega_0) + \frac{\tau_{3L}}{2}\end{vmatrix} = 0. \tag{3}$$

Separating the real and imaginary parts of the characteristic equation, we can get

$$\begin{cases}(\omega-\omega_0)\left[(\omega-\omega_0)^2 - \frac{1}{2}\omega_0^2 k_m^2 - \frac{\tau_{3L}}{2}\left(\frac{\tau_1}{2} - g\right)\right] = 0\\ \left(\frac{\tau_1}{2} + \frac{\tau_{3L}}{2} - g\right)\left[(\omega-\omega_0)^2 - \frac{1}{4}\omega_0^2 k_m^2\right] = 0.\end{cases} \tag{4}$$

The operating frequencies of the three-coil WPT relay system are obtained from the solutions of (4), which are described as follows:

Case 1: Exact PT-symmetric state.

In this case, the PT symmetry is exact. In order to ensure that the operating frequency ω is purely real, the coupling coefficient k_m has to satisfy the constraint condition that $k_m \geq k_C$. Here, k_C is the critical coupling coefficient, which can be derived as

$$k_C = \frac{\tau_{3L}}{\sqrt{2}\omega_0}. \tag{5}$$

From (5), it can be seen that the critical coupling coefficient k_C is determined by the load resistance and natural frequency of the coil, and it is $1/\sqrt{2}$ times of the critical coupling strength of the conventional second-order PT-symmetric WPT system [17], [18]. Thus, compared with the conventional PT-symmetric WPT system, the operating distance that the system maintains constant output power and transfer efficiency has been effectively improved.

Then, the gain coefficient g and operating frequency ω can be deduced as

$$\begin{cases} g = \frac{\tau_1 + \tau_{3L}}{2}\\ \omega = \omega_0 \pm \sqrt{\frac{1}{2}\omega_0^2 k_m^2 - \frac{1}{4}\tau_{3L}^2}.\end{cases} \tag{6}$$

By substituting (6) into (2), the amplitude of the modes $\boldsymbol{a}_1$ and $\boldsymbol{a}_3$ can be obtained as

$$|\boldsymbol{a}_1| = |\boldsymbol{a}_3| = \frac{V_\mathrm{s}}{\sqrt{L_1}(\tau_1 + \tau_{3L})}. \tag{7}$$

Thus, the output power P_out and transfer efficiency η of the system in this state can be derived as

$$P_\mathrm{out} = \tau_L|\boldsymbol{a}_3|^2 = \frac{\tau_\mathrm{L} V_\mathrm{s}^2}{L_1(\tau_1 + \tau_{3L})^2} \tag{8}$$

$$\eta = \frac{\tau_L|\boldsymbol{a}_3|^2}{\tau_1|\boldsymbol{a}_1|^2 + \tau_{3L}|\boldsymbol{a}_3|^2} = \frac{\tau_L}{\tau_1 + \tau_{3L}}. \tag{9}$$

From (8) and (9), it can be found that the power delivered to the load and the transfer efficiency only depend on the parameters of coils and the load resistance, and are independent of the coupling coefficient, which means that the system is robust to the variation of the transfer distance or misalignment in the strong coupling region ($k_\mathrm{m} \geq k_C$) to a certain extent.

Case 2: Broken PT-symmetric state.

At the critical coupling point k_C, the operating frequencies begin to undergo a bifurcation process and branch into two conjugate pairs, the PT symmetry is spontaneously broken. In the region ($\mathrm{k}_m < k_C$), the PT symmetry is broken, the corresponding gain coefficient g and operating frequency ω of the system are

$$\begin{cases} g = \frac{\tau_1}{2} + \frac{\omega_0^2 k_m^2}{2\tau_{3\mathrm{L}}}\\ \omega = \omega_0\left(1 \pm \frac{1}{2}k_m\right).\end{cases} \tag{10}$$

In this case, the amplitude of the modes $\boldsymbol{a}_1$ and $\boldsymbol{a}_3$ can be obtained as

$$|\boldsymbol{a}_1| = \frac{\tau_{3L} V_\mathrm{s}}{\sqrt{L_1}(\tau_1\tau_{3L} + \omega_0^2 k_m^2)} \tag{11}$$

$$|\boldsymbol{a}_3| = \frac{\omega_0 k_m}{\tau_{3L}}|\boldsymbol{a}_1| = \frac{\omega_0 k_m V_\mathrm{s}}{\sqrt{L_1}(\tau_1\tau_{3L} + \omega_0^2 k_m^2)}. \tag{12}$$

Then, the output power P_out and transfer efficiency η of the system in this state can be derived as

$$P_\mathrm{out} = \tau_\mathrm{L}|\boldsymbol{a}_3|^2 = \frac{\tau_\mathrm{L}\omega_0^2 k_m^2 V_\mathrm{s}^2}{L_1(\tau_1\tau_{3L} + \omega_0^2 k_m^2)^2} \tag{13}$$

$$\eta = \frac{\tau_L|\boldsymbol{a}_3|^2}{\tau_1|\boldsymbol{a}_1|^2 + \tau_{3L}|\boldsymbol{a}_3|^2} = \frac{\omega_0^2 k_\mathrm{m}^2 \tau_L}{\tau_{3\mathrm{L}}(\tau_1\tau_{3L} + \omega_0^2 k_m^2)}. \tag{14}$$

From (13) and (14), it can be observed that the output power and transfer efficiency depend on the coupling coefficient rather than remain constant.

Case 3: Resonant state.

In this case, the system works in the resonant state, which means that the operating frequency is equal to the natural

resonant frequency of the coil, i.e., $\omega = \omega_0$. Besides, the gain coefficient g exactly balances out the loss of the coils, i.e., $g = (\tau_1 + \tau_{3L})/2$. Substituting $\omega = \omega_0$ and $g = (\tau_1 + \tau_{3L})/2$ into (2), the amplitude of the modes $\boldsymbol{a}_1$ and $\boldsymbol{a}_3$ can be derived to be the same as (7). Then, the output power P_{out} and transfer efficiency η of the system in this state can be deduced to be the same as (8) and (9), respectively.

From the above analysis, it can be seen that the proposed WPT relay system with one repeater has three working states, and the system can automatically select a certain working state for stable operation at a certain transfer distance. In the exact PT-symmetric and resonant states, the output power and transfer efficiency are constant, which are independent of the coupling coefficient.

The same analysis can be extended to more than one repeater. For the systems with repeater numbers of 3, 5, 7,…, there are still three operating states, and output power and transfer efficiency of the system can remain constant against the variation of transfer distance in the exact PT-symmetric and resonant states. Generally, in the systems with an odd number of repeaters, it is not desirable to operate in the broken PT-symmetric state owing to the variable output power and transfer efficiency related to the coupling coefficient.

IV. Analysis of PT-Symmetric Model of System With an Even Number of Repeaters

Taking the WPT relay system with two repeaters as an example of an odd number of repeaters. Assuming that $\omega_1 \approx \omega_2 \approx \omega_3 \approx \omega_4 = \omega_0$, $r_2 \approx 0$, $r_3 \approx 0$, and $k_1 = k_3$, the dynamic equations of this four-coil WPT relay system can be written as

$$\frac{\mathrm{d}}{\mathrm{d}t}\begin{bmatrix}\boldsymbol{a}_1\\ \boldsymbol{a}_2\\ \boldsymbol{a}_3\\ \boldsymbol{a}_4\end{bmatrix} = \begin{bmatrix} \mathrm{j}\omega_0 - \frac{\tau_1}{2} + g & -\mathrm{j}\frac{\omega_0 k_1}{2} & 0 & 0\\ -\mathrm{j}\frac{\omega_0 k_1}{2} & \mathrm{j}\omega_0 & -\mathrm{j}\frac{\omega_0 k_2}{2} & 0\\ 0 & -\mathrm{j}\frac{\omega_0 k_2}{2} & \mathrm{j}\omega_0 & -\mathrm{j}\frac{\omega_0 k_1}{2}\\ 0 & 0 & -\mathrm{j}\frac{\omega_0 k_1}{2} & \mathrm{j}\omega_0 - \frac{\tau_{4L}}{2}\end{bmatrix}\begin{bmatrix}\boldsymbol{a}_1\\ \boldsymbol{a}_2\\ \boldsymbol{a}_3\\ \boldsymbol{a}_4\end{bmatrix}. \tag{15}$$

By calculating operating frequency, the real and imaginary parts of the characteristic equation can be separated as

$$\begin{cases} (\omega-\omega_0)^4 - (\omega-\omega_0)^2\left[\frac{\omega_0^2\left(2k_1^2+k_2^2\right)}{4} + \frac{\tau_{4L}}{2}\left(\frac{\tau_1}{2}-g\right)\right] \\ +\frac{\omega_0^2 k_2^2 \tau_{4L}}{8}\left(\frac{\tau_1}{2}-g\right) + \frac{\omega_0^4 k_1^4}{16} = 0 \\ (\omega-\omega_0)\left[(\omega-\omega_0)^2 - \frac{\omega_0^2\left(k_1^2+k_2^2\right)}{4}\right]\left(\frac{\tau_1}{2}+\frac{\tau_{4L}}{2}-g\right) = 0. \end{cases} \tag{16}$$

Then, the operating frequencies can be found as follows.

Case 1: Exact PT-symmetric state.

In this case, the gain coefficient g and operating frequency ω can be derived as (17) shown at the bottom of this page.

In order to ensure that all four operating frequencies are real, the coupling coefficient k_2 has to satisfy the constraint condition that $k_{\text{CL}} \le k_2 \le k_{\text{CH}}$. k_{CL} and k_{CH} are the critical coupling coefficients, which determines the effective distance that the system can transfer power stably, can be described as

$$\begin{cases} k_{\text{CL}} = k_1\sqrt{2\sqrt{1+\frac{2\tau_{4L}^2}{\omega_0^2 k_1^2}} - 2 - \frac{\tau_{4L}^2}{\omega_0^2 k_1^2}} \\ k_{\text{CH}} = \frac{\omega_0 k_1^2}{\tau_{4L}}. \end{cases} \tag{18}$$

Here, k_1 is assumed to be a definite value, which has to satisfy $k_1 \ge \tau_{4L}/(2\omega_0)$ to ensure that k_{CL} is real. If the coupling coefficients between adjacent coils are equal, i.e., $k_1 = k_2 = k_3$, the constraint condition of the coupling coefficients will degenerate into $k_2 \ge \tau_{4L}/\omega_0$.

As can be seen from (18), k_{CL} and k_{CH} are determined by the coupling coefficient between Tx (Rx) and Ix_1 (Ix_2) k_1, and k_{CL} determines the farthest boundary of the exact PT-symmetric region, which is always smaller than the critical coupling strength of the conventional second-order PT-symmetric WPT system [17], [18], and the degree of reduction is determined by k_1. Thus, by adjusting k_1, the transfer distance can be improved and regulated to meet specific application requirements.

Then, the amplitude of the modes $\boldsymbol{a}_1$ and $\boldsymbol{a}_4$ can be derived as

$$|\boldsymbol{a}_1| = |\boldsymbol{a}_4| = \frac{V_{\text{s}}}{\sqrt{L_1}\,(\tau_1+\tau_{4L})}. \tag{19}$$

Hence, the output power P_{out} and transfer efficiency η of the system in this state can be written as

$$P_{\text{out}} = \tau_{\text{L}}|\boldsymbol{a}_4|^2 = \frac{\tau_L V_{\text{s}}^2}{L_1(\tau_1+\tau_{4L})^2} \tag{20}$$

$$\eta = \frac{\tau_{\text{L}}|\boldsymbol{a}_4|^2}{\tau_1|\boldsymbol{a}_1|^2 + \tau_{4L}|\boldsymbol{a}_4|^2} = \frac{\tau_L}{\tau_1+\tau_{4L}}. \tag{21}$$

From (20) and (21), it can be seen that the four-coil WPT relay system can achieve constant output power and transfer efficiency against the varying transfer distances in the exact PT-symmetric region ($k_{\text{CL}} \le k_2 \le k_{\text{CH}}$).

Case 2: Broken PT-symmetric state.

In this case, if $k_1 \ne k_2$, the constraint conditions of k_2 are $k_2 < k_{\text{CL}}$ and $k_2 > k_{\text{CH}}$, but if $k_1 = k_2$, the restricted condition of k_2 will degenerate to $k_2 < \tau_{4L}/\omega_0$. The following analysis only considers the case of $k_1 \ne k_2$.

$$\begin{cases} g = \frac{\tau_1}{2} + \frac{\tau_{4L}}{2} \\ \omega = \omega_0\left[1 \pm \sqrt{\frac{1}{8}\left[\left(2k_1^2+k_2^2\right) - \frac{\tau_{4L}^2}{\omega_0^2} \pm \sqrt{4k_1^2\left(k_2^2 - \frac{\tau_{4L}^2}{\omega_0^2}\right) + \left(k_2^2 + \frac{\tau_{4L}^2}{\omega_0^2}\right)^2}\right]}\right] \end{cases} \tag{17}$$

The gain coefficient g and operating frequency ω can be derived as

$$\begin{cases} g = \frac{\tau_1}{2} + \frac{\omega_0^2 k_2^2}{2\tau_{4L}} \\ \omega = \omega_0 \left(1 \pm \frac{1}{2}\sqrt{k_1^2 + k_2^2}\right). \end{cases} \tag{22}$$

The amplitude of the modes $\boldsymbol{a}_1$ and $\boldsymbol{a}_4$ are

$$|\boldsymbol{a}_1| = \frac{\tau_{4L} V_s}{\sqrt{L_1}\left(\tau_1 \tau_{4L} + \omega_0^2 k_2^2\right)} \tag{23}$$

$$|\boldsymbol{a}_4| = \frac{\omega_0 k_2}{\tau_{4L}} |\boldsymbol{a}_1|. \tag{24}$$

Then, the output power P_{out} and transfer efficiency η of the system in this state can be obtained as

$$P_{\text{out}} = \tau_L |\boldsymbol{a}_4|^2 = \frac{\omega_0^2 k_2^2 \tau_L V_s^2}{L_1 (\tau_1 \tau_{4L} + \omega_0^2 k_2^2)^2} \tag{25}$$

$$\eta = \frac{\tau_L |\boldsymbol{a}_4|^2}{\tau_1 |\boldsymbol{a}_1|^2 + \tau_{4L} |\boldsymbol{a}_4|^2} = \frac{\omega_0^2 k_2^2 \tau_L}{(\tau_1 \tau_{4L} + \omega_0^2 k_2^2)\tau_{4L}}. \tag{26}$$

Case 3: Resonant state.

In this case, the system works in the resonant state, the operating frequency is located at $\omega = \omega_0$, and the gain coefficient g can be deduced as

$$g = \frac{\tau_1}{2} + \frac{\omega_0^2 k_1^4}{2k_2^2 \tau_{4L}}. \tag{27}$$

The amplitude of the modes $\boldsymbol{a}_1$ and $\boldsymbol{a}_4$ can be written as

$$|\boldsymbol{a}_1| = \frac{k_2^2 \tau_{4L} V_s}{\sqrt{L_1}\left(k_2^2 \tau_1 \tau_{4L} + \omega_0^2 k_1^4\right)} \tag{28}$$

$$|\boldsymbol{a}_4| = \frac{\omega_0 k_1^2}{k_2 \tau_{4L}} |\boldsymbol{a}_1|. \tag{29}$$

Then, the output power P_{out} and transfer efficiency η of the system in this state can be derived as

$$P_{\text{out}} = \tau_L |\boldsymbol{a}_4|^2 = \frac{\omega_0^2 k_1^4 k_2^2 \tau_L V_s^2}{L_1 (k_2^2 \tau_1 \tau_{4L} + \omega_0^2 k_1^4)^2} \tag{30}$$

$$\eta = \frac{\tau_L |\boldsymbol{a}_4|^2}{\tau_1 |\boldsymbol{a}_1|^2 + \tau_{4L} |\boldsymbol{a}_4|^2} = \frac{\omega_0^2 k_1^4 \tau_L}{(k_2^2 \tau_1 \tau_{4L} + \omega_0^2 k_1^4)\tau_{4L}}. \tag{31}$$

From the above analysis, it can be seen that the proposed WPT relay system with two repeaters achieves constant output power and near-unity transfer efficiency in the exact PT-symmetric state. Once the transfer distance exceeds the constraints, the system will work in the broken PT-symmetric or resonant state. The output power and transfer efficiency will vary with the transfer distance, which is different from the systems with an odd number of repeaters.

The same analysis can be extended to the system with repeater numbers of 6, 8, 10, ... In general, in systems with an even number of repeaters, it is not desirable to operate in the broken PT-symmetric state and resonant state due to the variable output power and transfer efficiency related to the coupling coefficient.

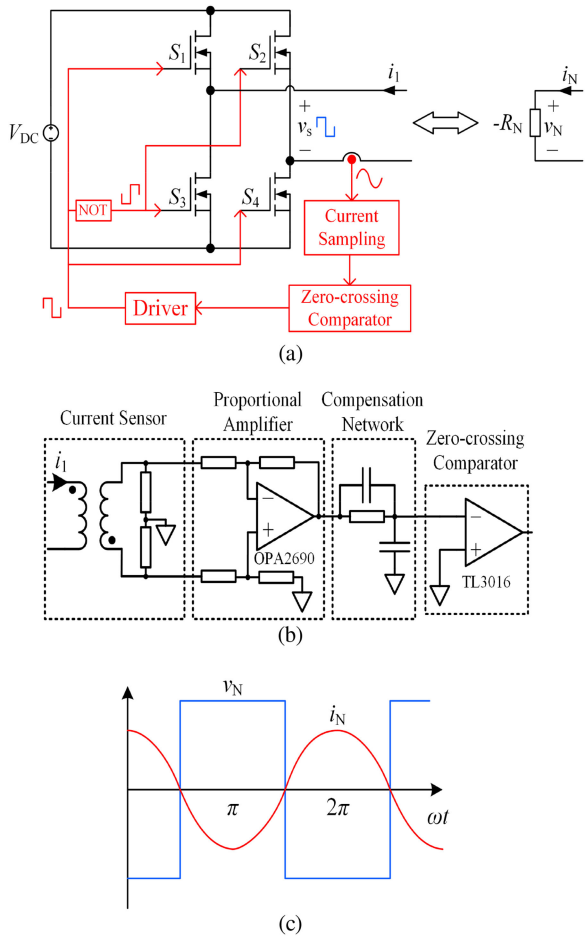

Fig. 2. Negative resistance $-R_N$ implementation. (a) Full-bridge inverter realizing $-R_N$. (b) Control circuit of $-R_N$. (c) Voltage and current of $-R_N$ in the steady state.

V. Experimental Verification

A. Negative Resistance Implementation

The negative resistance is essential for the operation of the proposed relay system with constant output power and transfer efficiency. It is an active device that obeys Ohm's law, its current flows backward from low voltage to high voltage, and its volt–ampere characteristic curve is a negatively sloped line [23].

Fig. 2(a) shows the circuit of a full-bridge inverter for realizing a negative resistance $-R_N$. The control circuit is shown in Fig. 2(b), in which the current of Tx is used as the feedback signal to generate the driving signals of the switches $S_1 \sim S_4$. The zero-crossing comparator keeps the phase difference between the output voltage and current of the full-bridge at 180°, thereby realizing the voltage–current characteristic of the negative resistance, as shown in Fig. 2(c).

Moreover, the fundamental component of the output voltage of the full-bridge inverter can be derived as

$$V_s = \frac{2\sqrt{2} V_{\text{dc}}}{\pi}. \tag{32}$$

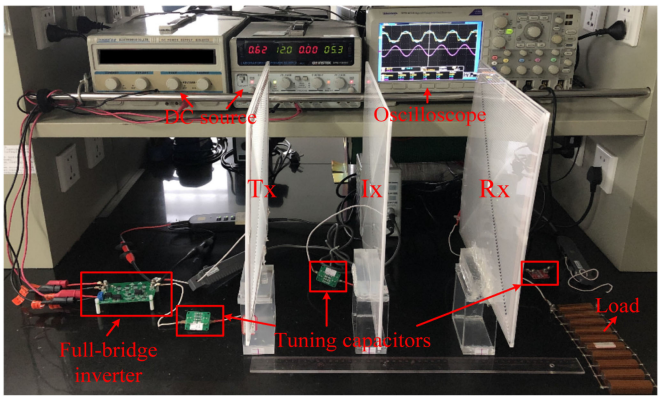

Fig. 3. Experimental prototype of the proposed PT-symmetric-based WPT system with a repeater.

TABLE I
PARAMETERS OF THE PROTOTYPE

Symbol	Description	Values
V_{DC}	DC source voltage	15V
L_1	Inductance of Tx	15.48μH
L_2	Inductance of Ix_1	15.47μH
L_3	Inductance of Ix_2	15.50μH
L_4	Inductance of Rx	15.52μH
C_1	Tuning capacitance of Tx	1.67nF
C_2	Tuning capacitance of Ix_1	1.67nF
C_3	Tuning capacitance of Ix_2	1.66nF
C_4	Tuning capacitance of Rx	1.66nF
r_1	Parasitic resistance of Tx	245.66mΩ
r_2	Parasitic resistance of Ix_1	243.95mΩ
r_3	Parasitic resistance of Ix_2	208.21mΩ
r_4	Parasitic resistance of Rx	222.16mΩ
R_L	Equivalent load resistance	10Ω

B. System Implementation

Fig. 3 shows the experimental prototype. The size of each coil is 320 mm × 320 mm, and the coils are fabricated by using Φ0.05 mm*800 silk covered wire with the turn spacing of 1.4 mm. All measured electrical parameters of the prototype are listed in Table I, which are obtained by the precise impedance analyzer (Wayne Kerr 6500B).

Based on the theoretical analysis in Sections III and IV, for the one-repeater system, the critical coupling coefficient k_C can be calculated as 0.0748. Similarly, for the two-repeater system, the coupling coefficient k_1 has to satisfy $k_1 \geq 0.0529$. Here, considering that the exact PT-symmetric region ($k_{CL} \leq k_2 \leq k_{CH}$) is determined by k_1, we assume that k_1 is 0.12, then the critical coupling coefficients k_{CL} and k_{CH} can be calculated as 0.0777 and 0.1362, respectively. Therefore, the effective range that the system maintains constant output power and constant transfer efficiency is limited to $0.0777 \leq k_2 \leq 0.1362$.

C. Experimental Results and Discussion

The values of mutual inductance between two adjacent coils were measured by the precise impedance analyzer (Wayne Kerr 6500B). Fig. 4(a) shows the variation curves of coupling coefficients (k_1, k_2) with the center-to-center distance of the coils in the one-repeater system, from which the critical distance corresponding to $k_C = 0.0748$ is near 210 mm for the coaxial aligned case. Therefore, the critical transfer distance d_{13} between Tx and Rx is near 420 mm. Fig. 4(b) depicts the relationship curves between the coupling coefficients (k_1, k_2, k_3) and the center-to-center distance of the coils in the two-repeater system. Here, k_1 (k_3) is set as 0.12, which corresponds to the distance d_{12} (d_{34}) ≈150 mm for the coaxial aligned case. And the range of transfer distance d_{23} corresponding to k_2 is about 120 mm ≤ d_{23} ≤ 200 mm. Thus, the critical region of the transfer distance d_{14} between Tx and Rx is about 420 mm ≤ d_{14} ≤ 500 mm.

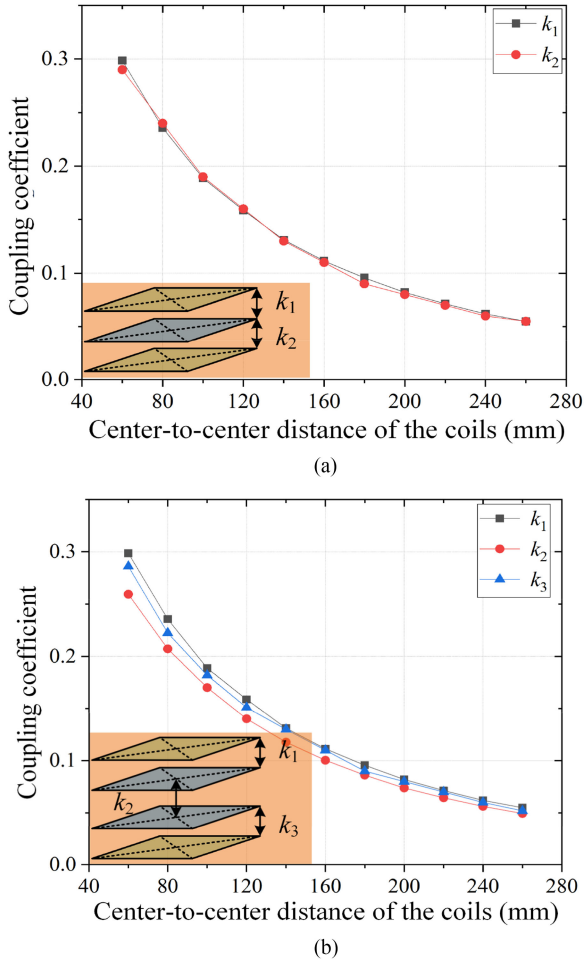

Fig. 4. Measured results of coupling coefficient versus center-to-center distance between two adjacent coils for the coaxial aligned case. (a) k_1 and k_2 in the one-repeater system. (b) k_1, k_2, and k_3 in the two-repeater system.

Fig. 5 shows the operational waveforms of the one-repeater prototype when the Rx is placed in different positions within the exact PT-symmetric region. Based on the theoretical analysis in Section III, in the exact PT-symmetric region, the system automatically operates in the exact PT-symmetric state or the resonant state, in which the output power and transfer efficiency of the proposed system remain constant. When the relative positions of Tx and Rx are 1) $d_{13} = 240$ mm, 2) $d_{13} = 320$ mm, and 3) $d_{13} = 400$ mm, the rms values of the currents i_1 and i_3 are equal, respectively, typically resulting in constant output power and invariant transfer efficiency. The experimental measured data of output power P_{out}, transfer efficiency η and operating

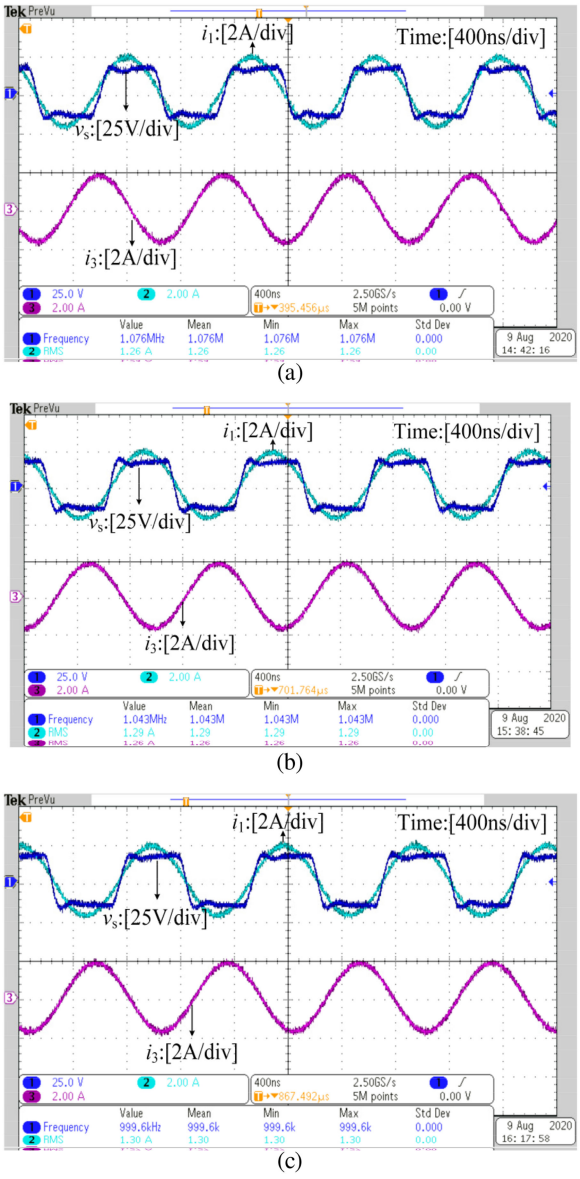

Fig. 5. Operation waveforms of the one-repeater prototype when the three coils are coaxial aligned. (a) $d_{13} = 240$ mm. (b) $d_{13} = 320$ mm. (c) $d_{13} = 400$ mm.

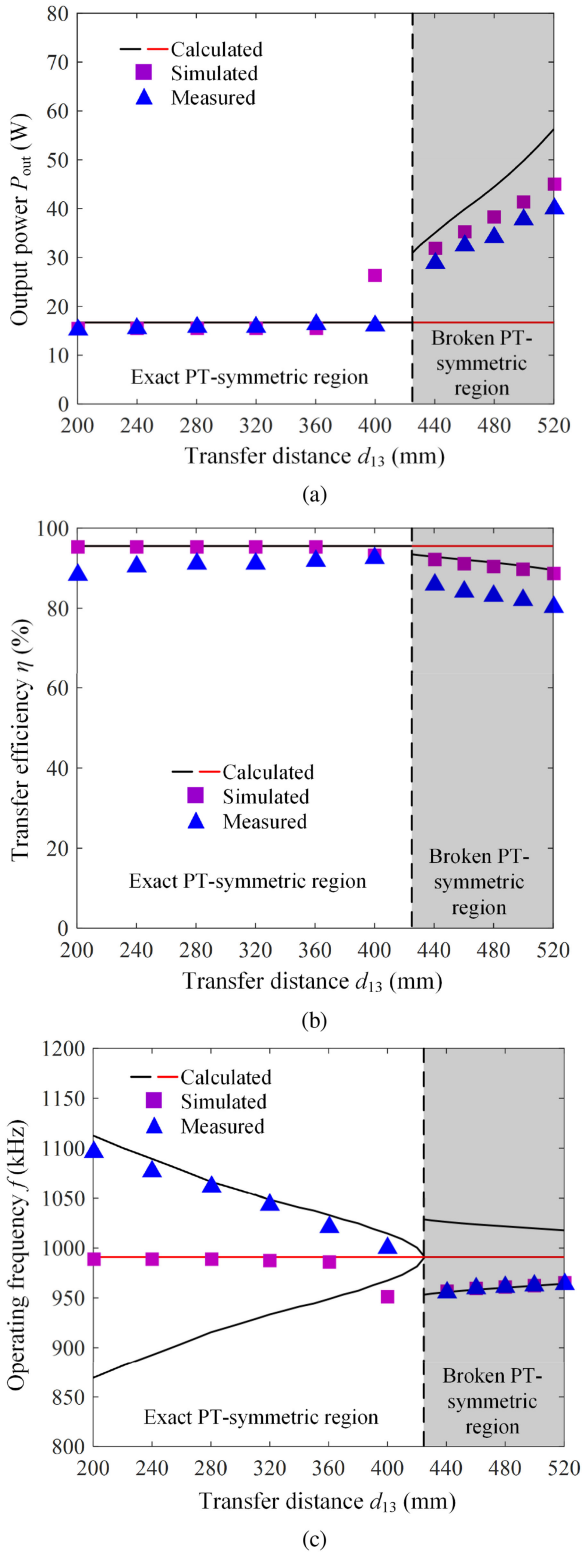

Fig. 6. Transfer performance of the one-repeater prototype for the coaxial aligned case. (a) Output power $P_{\rm out}$ versus the transfer distance d_{13}. (b) Transfer efficiency η versus the transfer distance d_{13}. (c) Operating frequency ω versus the transfer distance d_{13}.

frequency f are described in Fig. 6. The solid lines represent the theoretical calculated curves, the purple square discrete points denote the simulated values, and the blue triangular discrete points represent the experimental measured results.

As can be seen from Fig. 6, the output power and transfer efficiency of the one-repeater system remain constant within a range of about 420 mm. In this region, the output power of the one-repeater prototype is nearly stable at 15 W, and the transfer efficiency is constant near 91%. When the transfer distance exceeds 420 mm, the output power and transfer efficiency of the prototype are dependent on the variation of the transfer distance and do not remain constant, which is not desirable. Besides, as is illustrated in Fig. 6(c), the operating frequency of the one-repeater system has three real solutions in the exact PT-symmetric region ($k_{\rm m} \geq k_C$) and broken PT-symmetric region ($k_m < k_C$). Here, in the range of $d_{13} > 420$ mm, the one-repeater prototype automatically works in the exact PT-symmetric state, but for the range of $d_{13} < 420$ mm, the prototype operates in the

TABLE II
OUTPUT POWER AND TRANSFER EFFICIENCY OF THE EXPERIMENTAL ONE-REPEATER PROTOTYPE

d_{13} (mm)	Exact PT-symmetric region						Broken PT-symmetric region				
	200	240	280	320	360	400	440	460	480	500	520
Calculated P_{out} (W)	16.69	16.69	16.69	16.69	16.69	16.69	35.00	39.86	44.48	49.89	56.26
Measured P_{out} (W)	15.13	15.38	15.88	15.88	16.38	16.13	28.75	32.45	34.18	37.86	41.95
Relative error	-9.35%	-7.85%	-4.85%	-4.85%	-1.86%	-3.36%	-17.86%	-18.59%	-23.16%	-24.11%	-25.44%
Calculated η (%)	95.53	95.53	95.53	95.53	95.53	95.53	92.86	92.13	91.42	90.57	89.55
Measured η (%)	88.24	90.39	91.16	91.16	91.94	92.62	85.77	84.21	83.15	81.95	80.41
Relative error	-7.63%	-5.38%	-4.57%	-4.57%	-3.76%	-3.05%	-7.64%	-8.60%	-9.05%	-9.52%	-10.21%

TABLE III
OUTPUT POWER AND TRANSFER EFFICIENCY OF THE EXPERIMENTAL TWO-REPEATER PROTOTYPE

d_{14} (mm)	Broken PT-symmetric region			Exact PT-symmetric region				Broken PT-symmetric region		
	400	410	420	440	460	480	500	510	520	530
Calculated P_{out} (W)	25.35	21.59	17.60	16.69	16.69	16.69	32.48	35.90	40.95	45.75
Measured P_{out} (W)	26.75	20.45	15.38	15.88	15.88	15.88	15.63	29.33	31.03	31.26
Relative error	5.52%	-5.28%	-12.61%	-4.85%	-4.85%	-4.85%	-51.88%	-18.3%	-24.22%	-31.67%
Calculated η (%)	94.28	94.83	95.40	95.53	95.53	95.53	93.24	92.73	91.96	91.22
Measured η (%)	90.26	89.78	85.64	89.77	87.76	89.09	87.68	86.64	84.00	82.18
Relative error	-4.26%	-5.33%	-10.23%	-6.03%	-8.13%	-6.74%	-5.96%	-6.57%	-8.66%	-9.91%

broken PT-symmetric state, the measured operating frequencies are in good agreement with the calculated results. To sum up, for the one-repeater prototype, the output power and transfer efficiency always remain constant against the variation of the coupling coefficient in the exact PT-symmetric region, no matter the system works in the exact PT-symmetric state or the resonant state.

Furthermore, the calculated and measured values of the output power and transfer efficiency and their differences in percentage are listed in Table II. Considering that the coupled-mode approach is an approximate method, and the internal resistance of the repeater exists in the actual circuit, the errors between experimental results and theoretical analysis are in an acceptable range. More detailed error analysis is elaborated at the end of this section.

Fig. 7 shows the operational waveforms of the two-repeater prototype when the Rx is placed in different positions within the exact PT-symmetric region, in which the four coils are coaxial aligned. According to the equal rms values of the currents i_1 and i_4 at different relative positions: 1) $d_{14} =$ 420 mm, 2) $d_{14} = 460$ mm, and 3) $d_{14} = 500$ mm between Tx and Rx, it can be easily judged that the proposed system works in the exact PT-symmetric state, in which the output power and transfer efficiency of the proposed system remain constant.

Fig. 8 depicts the experimental measured data of output power $P_{\rm out}$, transfer efficiency η, and operating frequency f. The calculated and measured values of the output power and transfer efficiency and their differences in percentage are listed in Table III. It is noted that the relative error of the output power at position $d_{14} = 500$ mm is very large because this position is near the critical position, and due to the slight variations of the actual parameters in the experiment, the system works in the exact PT-symmetric state. The detailed error analysis is elaborated at the end of this section.

As is illustrated in Fig. 8, the two-repeater prototype achieves a stable power transfer of about 15 W with a constant transfer efficiency of approximately 89% within a range of about 420–500 mm air gap. In this region, the operating frequency of the system has five real solutions, and the system works on a certain operating frequency branch. Here, the two-repeater prototype automatically works in the exact PT-symmetric state, in which the output power and transfer efficiency are independent of the transfer distance. While in the broken PT-symmetric region ($d_{14} > 500$ mm and $d_{14} < 420$ mm), the prototype works in the broken PT-symmetric state or the resonant state, in which both output power and transfer efficiency vary with different transfer distance, which is not desirable. Therefore, for the two-repeater system, it is desired that the system operates in the PT-symmetric region, in which the output power and transfer efficiency can maintain constant against the variation of the transfer distance.

As can be observed from Figs. 6 and 8, there are discrepancies between the theoretical analysis and experimental results, but it is acceptable and does not affect the validity of the theoretical analysis. The main reasons are summarized as follows: First, the coupled-mode approach is an approximate method, the coupled-mode approximation conditions including equal natural frequencies of coils, high quality factors, and weak coupling coefficients [33]–[35] are not always strictly satisfied in the experiments. Second, for a high-order PT-symmetric WPT system, the coupled-mode equation of the system must satisfy the

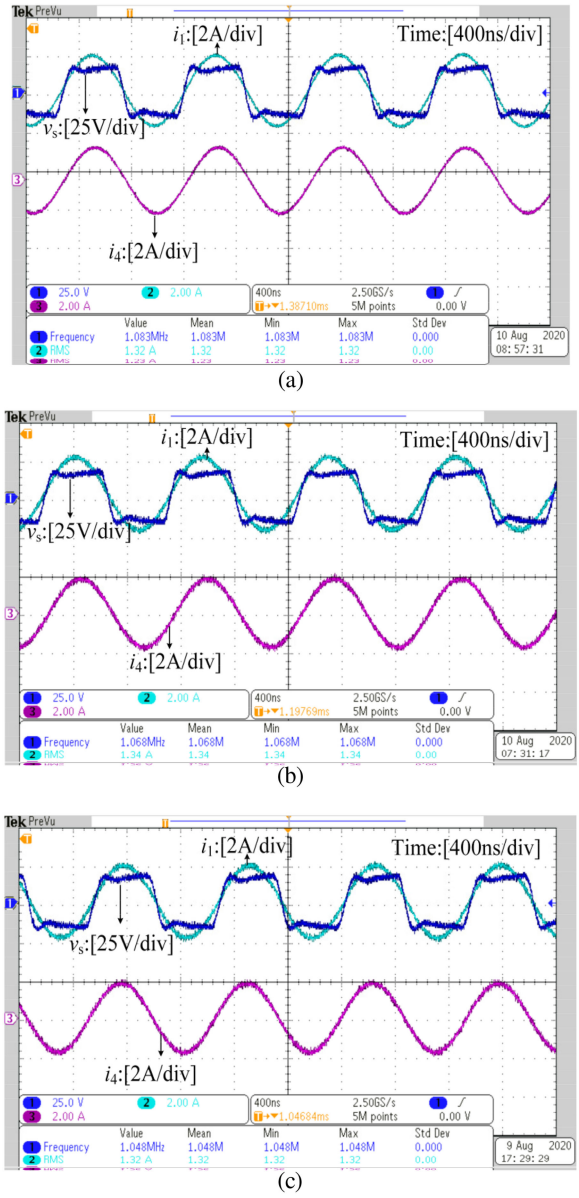

Fig. 7. Operation waveforms of the two-repeater prototype when the four coils are coaxial aligned. (a) $d_{14} = 420$ mm. (b) $d_{14} = 460$ mm. (c) $d_{14} = 500$ mm.

PT-symmetric conditions to achieve PT symmetry [23], but there are some deviations in the experiments. Last, in the experiment, the natural frequencies of coils are slightly shifted due to the positions of coils and the movement of transfer distance, and the coupling coefficients between adjacent coils are slightly different due to measurement errors. Besides, the internal resistances of the repeaters are inevitable in the actual circuit. The farther the transfer distance is, the more obvious the influence of the internal resistances on the transfer characteristics will be.

D. Comparison With Existing WPT Relay Systems

Table IV compares transfer performances of existing WPT systems with one and two repeaters published in recent years.

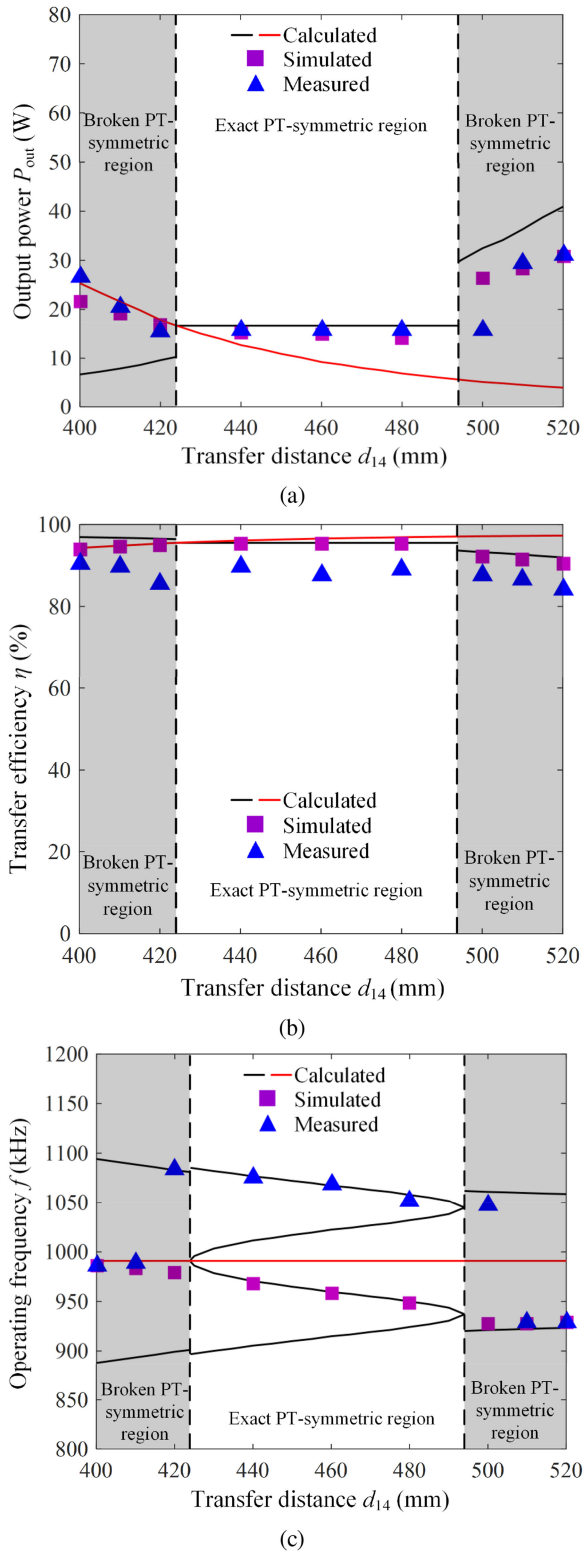

Fig. 8. Transfer performance of the two-repeater prototype for the coaxial aligned case. (a) Output power P_{out} versus the transfer distance d_{14}. (b) Transfer efficiency η versus the transfer distance d_{14}. (c) Operating frequency ω versus the transfer distance d_{14}.

According to Table IV, the PT-symmetric WPT relay system with multiple repeaters proposed in this article has competitive advantages.

TABLE IV
COMPARISON OF EXISTING WPT SYSTEMS

Ref.	Coils	Frequency (kHz)	Distance (mm)	Power (W)	Efficiency (%)	Operating condition
[24]	3	99	242	1000	87.5	Fixed
[25]	3	200	100	15.2	95.6	Fixed
[27]	3	115.6	30	5.61	61.4	Fixed
[29]	3	6780	200	--	65	Fixed
[30]	4	90	200	3300	96.56	Fixed
[31]	4	4630	450	3.1	72.4	Fixed
This	3	991	420	15	91	Variable
paper	4	991	500	15	89	Variable

VI. CONCLUSION

In this article, a robust extended-distance WPT system with multiple repeaters based on the concept of PT symmetry was proposed, in which the generalized PT-symmetric model for the multirepeater WPT system was presented to evaluate the benefits of the proposed system. The major contributions of this article are as follows.

1) We propose the PT-symmetric WPT system with any number of repeaters, and verify the difference between odd and even number of repeaters to operate in PT symmetry, which is useful to extend the transfer distance.
2) We find that the critical coupling coefficient of the PT-symmetric WPT system with any number of repeaters is reduced, which improves the maximum transfer distance of the PT-symmetric region.
3) For the even number of repeaters, the output power and transfer efficiency can remain constant against the variation of the coupling coefficient in the exact PT-symmetric region without maintaining $k_1 = k_2$, which indicates that the system is robust against the misalignments and variations in the transfer distance.
4) For the odd number of repeaters, the operating frequency of the system in the resonant state is fixed, and the output power and transfer efficiency can be kept constant in the near-field range. Besides, the system effectively overcomes the frequency splitting phenomenon of the existing MCR-WPT system in the strong coupling region.

Based on the PT-symmetric model, the multirepeater WPT system can achieve stable output power and constant transfer efficiency that are independent of transfer distance variation in the exact PT-symmetric region. To verify the transfer performances of the PT-symmetric-based multi-repeater WPT system, a 15-W prototype was implemented and tested. The experimental results validate the theoretical analysis.

REFERENCES

[1] A. Kurs, A. Karalis, R. Moffatt, J. D. Joannopoulos, P. Fisher, and M. Soljacic, "Wireless power transfer via strongly coupled magnetic resonances," *Science*, vol. 317, no. 5834, pp. 83–86, Jul. 2007.

[2] P. Riehl *et al.*, "Wireless power systems for mobile devices supporting inductive and resonant operating modes," *IEEE Trans. Microw. Theory Techn.*, vol. 63, no. 3, pp. 780–790, Mar. 2015.

[3] H. H. Lee, S. H. Kang, and C. W. Jung, "MR-WPT with reconfigurable resonator and ground for laptop application," *IEEE Microw. Wireless Compon. Lett.*, vol. 28, no. 3, pp. 269–271, Mar. 2018.

[4] S. Y. R. Hui, "Planar wireless charging technology for portable electronic products and qi," *Proc. IEEE*, vol. 101, no. 6, pp. 1290–1301, Jun. 2013.

[5] J. Shin, S. Shin, Y. Kim, S. Ahn, and S. Lee, "Design and implementation of shaped magnetic-resonance-based wireless power transfer system for roadway-powered moving electric vehicles," *IEEE Trans. Ind. Electron.*, vol. 61, no. 3, pp. 1179–1192, Mar. 2014.

[6] G. Buja, M. Bertoluzzo, and H. K. Dashora, "Lumped track layout design for dynamic wireless charging of electric vehicles," *IEEE Trans. Ind. Electron.*, vol. 63, no. 10, pp. 6631–6640, Oct. 2016.

[7] A. Ahmad, M. S. Alam, and R. Chabaan, "A comprehensive review of wireless charging technologies for electric," *IEEE Trans. Transp. Electrific.*, vol. 4, no. 1, pp. 38–63, Mar. 2018.

[8] A. Kush, J. Rangarajan, Y. X. Guo, and N. V. Thakor, "Wireless power transfer strategies for implantable bioelectronics," *IEEE Rev. Biomed. Eng.*, vol. 10, pp. 136–161, Mar. 2017.

[9] D. Ahn and S. Hong, "Wireless power transmission with self-regulated output voltage for biomedical implant," *IEEE Trans. Ind. Electron.*, vol. 61, no. 5, pp. 2225–2235, May 2014.

[10] G. Sun, B. Muneer, Y. Li, and Q. Zhu, "Ultracompact implantable design with integrated wireless power transfer and RF transmission capabilities," *IEEE Trans. Biomed. Circuits Syst.*, vol. 12, no. 2, pp. 281–291, Apr. 2018.

[11] S. Zhang, Z. Qian, J. Wu, F. Kong, and S. Lu, "Wireless charger placement and power allocation for maximizing charging quality," *IEEE Trans. Mob. Comput.*, vol. 17, no. 6, pp. 1483–1496, Jun. 2018.

[12] Q. Li and Y. C. Liang, "An inductive power transfer system with a high-Q resonant tank for mobile device charging," *IEEE Trans. Power Electron.*, vol. 30, no. 11, pp. 6203–6212, Nov. 2015.

[13] T.-D. Yeo, D. Kwon, S.-T. Khang, and J.-W. Yu, "Design of maximum efficiency tracking control scheme for closed-loop wireless power charging system employing series resonant tank," *IEEE Trans. Power Electron.*, vol. 32, no. 1, pp. 471–478, Jan. 2017.

[14] P. K. S. Jayathurathnage, A. Alphones, and D. M. Vilathgamuwa, "Optimization of a wireless power transfer system with a repeater against load variations," *IEEE Trans. Ind. Electron.*, vol. 64, no. 10, pp. 7800–7809, Oct. 2017.

[15] J. Lee, K. Lee, and D. Cho, "Stability improvement of transmission efficiency based on a relay resonator in a wireless power transfer system," *IEEE Trans. Power Electron. Lett.*, vol. 32, no. 5, pp. 3297–3300, May 2017.

[16] B. N. Wang, K. H. Teo, T. Nishino, W. Yerazuins, J. Barnwell, and J. Zhang, "Experiments on wireless power transfer with metamaterials," *Appl. Phys. Lett.*, vol. 98, no. 25, Jun. 2011, Art. no. 254101.

[17] S. Assawaworrarit, X. Yu, and S. Fan, "Robust wireless power transfer using a nonlinear parity-time-symmetric circuit," *Nature*, vol. 546, pp. 387–390, Jun. 2017.

[18] J. Zhou, B. Zhang, W. Xiao, D. Qiu, and Y. Chen, "Nonlinear parity-time symmetric model for constant efficiency wireless power transfer: Application to a Drone-in-Flight wireless charging platform," *IEEE Trans. Ind. Electron.*, vol. 66, no. 5, pp. 4097–4107, May 2019.

[19] C. M. Bender, S. Boettcher, and P. N. Meisinger, "PT-symmetric quantum mechanics," *J. Math. Phys.*, vol. 40, no. 5, pp. 2201–2229, May 1999.

[20] S. K. Ozdemir, S. Rotter, F. Nori, and L. Yang, "Parity-time symmetry and exceptional points in photonics," *Nature Mater.*, vol. 18, no. 8, pp. 783–798, Apr. 2019.

[21] M. A. Miri and A. Alu, "Exceptional points in optics and photonics," *Science*, vol. 363, pp. 1–11, Jan. 2019.

[22] R. Fleury, D. L. Sounas, and A. Alu, "Parity-time symmetry in acoustics: Theory, devices, and potential applications," *IEEE J. Sel. Topics Quant. Electron.*, vol. 22, no. 5, Sep. 2016, Art. no. 5000809.

[23] J. Schindler, Z. Lin, J. M. Lee, H. Ramezani, F. M. Ellis, and T. Kottos, "PT-symmetric electronics," *J. Phys. A: Math. Theory*, vol. 45, pp. 1–17, Sep. 2012.

[24] K.-K. Oh, "Design and voltage regulation of inductively coupled wireless power transfer circuits with an intermediate coil," *IET Power Electron.*, vol. 12, no. 13, pp. 3488–3498, Nov. 2019.

[25] F. Wen, X. Chu, Q. Li, R. Li, L. L, and F. Jing, "Optimization on three-coil long-range and dimension-asymmetric wireless power transfer system," *IEEE Trans. Electromagn. Compat.*, vol. 62, no. 5, pp. 1859–1868, Oct. 2020.

[26] J. Kim, H.-C. Con, K.-H. Kim, and Y.-J. Park, "Efficiency analysis of magnetic resonance wireless power transfer with intermediate resonant coil," *IEEE Antennas Wireless Propag. Lett.*, vol. 10, pp. 389–392, May 2011.

[27] W. X. Zhong, C. Zhang, X. Liu, and S. Y. R. Hui, "A methodology for making a three-coil wireless power transfer system more energy efficient than a two-coil counterpart for extended transfer distance," *IEEE Trans. Power Electron.*, vol. 30, no. 2, pp. 933–942, Feb. 2015.

[28] J. Zhang, X. Yuan, C. Wang, and Y. He, "Comparative analysis of two-coil and three-coil structures for wireless power transfer," *IEEE Trans. Power Electron.*, vol. 32, no. 1, pp. 341–352, Jan. 2017.
[29] D.-W. Seo, "Comparative analysis of two- and three-coil WPT systems based on transmission efficiency," *IEEE Access*, vol. 7, pp. 151962–151970, Oct. 2019.
[30] S. Moon and G.-W. Moon, "Wireless power transfer system with an asymmetric four-coil resonator for electric vehicle battery chargers," *IEEE Trans. Power Electron.*, vol. 31, no. 10, pp. 6844–6854, Oct. 2016.
[31] X. Liu and G. Wang, "A novel wireless power transfer system with double intermediate resonant coils," *IEEE Trans. Ind. Electron.*, vol. 63, no. 4, pp. 2174–2180, Apr. 2016.
[32] H. Li, K. Wang, L. Huang, W. Chen, and X. Yang, "Dynamic modeling based on coupled modes for wireless power transfer systems," *IEEE Trans. Power Electron.*, vol. 30, no. 11, pp. 6245–6253, Nov. 2015.
[33] W. H. Louisell, *Coupled Mode and Parametric Electronics*. New York, NY, USA: Wiley, 1960.
[34] H. A. Haus, *Waves and Fields in Optoelectronics*. Englewood Cliffs, NJ, USA: Prentice-Hall, 1984, pp. 197–216.
[35] M. Kiani and M. Ghovanloo, "The circuit theory behind coupled-mode magnetic resonance-based wireless power transmission," *IEEE Trans. Circuits Syst. I, Regular Papers*, vol. 59, no. 9, pp. 2065–2074, Sep. 2012.

Xujian Shu was born in Anhui, China, in 1993. She received the B.S. degree in electrical engineering and automation from China University of Mining and Technology, Xuzhou, China, in 2015. She is currently working toward the Ph.D. degree in power electronics with the School of Electric Power, South China University of Technology, Guangzhou, China.

Her research interests include wireless power transfer applications and power electronics converters.

Bo Zhang (Senior Member, IEEE) was born in Shanghai, China, in 1962. He received the B.S. degree in electrical engineering from Zhejiang University, Hangzhou, China, in 1982, the M.S. degree in power electronics from Southwest Jiaotong University, Chengdu, China, in 1988, and the Ph.D. degree in power electronics from Nanjing University of Aeronautics and Astronautics, Nanjing, China, in 1994.

He is currently a Professor with the School of Electric Power, South China University of Technology, Guangzhou, China. He has authored or coauthored more than 450 papers and held 102 patents. He has authored eight monographs. His research interests include nonlinear analysis and control of power electronics, wireless power transfer technology, and ac drives.

Zhihao Wei was born in Shandong, China, in 1990. He received the B.S. and M.S. degrees in electrical engineering from Qingdao University, Qingdao, China, in 2015, 2018, respectively. He is currently working toward the Ph. D. degree in power electronics and power drives with the School of Electric Power, South China University of Technology, Guangzhou, China.

His research interests include wireless power transmission technology and fractional-order system.

Chao Rong was born in Shanxi, China, in 1995. He received the B.S. degree in electrical engineering and automation in 2018 from the South China University of Technology, Guangzhou, China, where he is currently working toward the Ph.D. degree in power electronics and power drives.

His research interests include wireless power transfer technology.

Shubin Sun was born in Chaozhou, Guangdong, China, in 1994. He received the B.S. degree in electrical engineering from Nanjing University of Science and Technology, Nanjing, China, in 2018. He is currently working toward the M.S. degree in power electronic with the School of Electric Power, South China University of Technology, Guangzhou, China.

His research interests include wireless power transfer applications and power converter applications.